Direct Observation of Orbital Magnetism in Cubic Solids

W. D. Brewer,[1,*] A. Scherz,[1] C. Sorg,[1] H. Wende,[1] K. Baberschke,[1] P. Bencok,[2] and S. Frota-Pessôa[3]

[1]*Institut für Experimentalphysik, Freie Universität Berlin, Arnimallee 14, D-14195 Berlin-Dahlem, Germany*

[2]*European Synchrotron Radiation Facility, BP 220, F-38043 Grenoble Cedex, France*

[3]*Instituto de Física, Universidade de São Paulo, CP 66318, 05315-970 São Paulo, São Paulo, Brazil*

(Received 17 September 2003; published 11 August 2004)

We present x-ray magnetic circular dichroism determinations of the orbital/spin magnetic moment ratios of dilute 3*d*-series impurities in Au (and Cu) host matrices. This is the first direct measurement of considerable orbital moments in cubic symmetry for a localized impurity in a bulk metal host. It is shown that the unquenching of orbital magnetism depends on a delicate balance of hybridization effects between the local impurity with the host and the filling of the 3*d* states of the impurity. The results are accompanied by *ab initio* calculations that support our experimental findings.

DOI: 10.1103/PhysRevLett.93.077205 PACS numbers: 75.20.Hr, 78.20.Ls, 78.70.Dm

Magnetism of localized and isolated magnetic moments, in particular, in cubic symmetry in metal hosts, has been a major field of research in the past and is described in many textbooks. The Kondo effect, pair breaking in superconductors, Friedel and RKKY oscillations, spin polarization, etc., have been investigated and theoretically interpreted in great detail [1,2]. At first glance it would seem that most of the magnetic properties are governed by spin magnetism and can be successfully explained by the coupling of the spin moment, S, of a local impurity to that of the conduction band, σ. This is in accordance with the discussions in many textbooks where the orbital moment is assumed to be quenched ($\langle L_z \rangle \equiv 0$) due to cubic or higher symmetry. On the other hand, strong orbital magnetism is exhibited by 3*d* ions as adatoms on surfaces, in clusters, and in nanostructures [3,4], which is in accordance with the unquenching of the orbital moment in lower symmetry. As mentioned above, for certain mechanisms, the spin moment of a magnetic impurity and its coupling in a Kondo-like Hamiltonian ($JS \cdot \sigma$) does indeed explain many results such as pair breaking, Kondo effect, etc. But concerning the magnetic anisotropy (MA) of soft and hard magnets, it is now clear that the orbital moments play a vital role. The reminiscence of orbital magnetism (nonspherical charge distribution) produces a magnetic anisotropy energy via spin-orbit coupling, while pure spin magnetism with $JS \cdot \sigma$ yields only soft magnets (no MA).

Since the 1970s, there have been indications that orbital magnetism of 3*d* impurities may survive in cubic symmetry [5–8]. However, in these studies the orbital moment was indirectly detected by means of the hyperfine coupling to the atomic nuclei, and thus no direct and quantitative spectroscopic observation of the orbital magnetic moment has been reported so far. The well-established x-ray magnetic circular dichroism (XMCD) method is most appropriate for measuring directly the orbital moments in a valence shell. However, due to intensity limitations of available sources, experiments were until recently limited to relatively concentrated systems. Only with the advent of the third generation synchrotron facilities (such as the ESRF) in combination with high magnetic fields of several Tesla has the study of the orbital and spin moments in a direct spectroscopic measurement of dilute 3*d* impurities become feasible. Here, we report the first observation of the x-ray absorption spectra (XAS) and XMCD in dilute alloys of 3*d* elements in a Au lattice, the classical system for the study of the formation of local moments in metal hosts. These dilute 3*d* impurities in noble metal hosts, as can be seen in the XAS spectra of the 3*d* impurities, represent an intermediate case between the atomic or nearly atomic configuration [3] and a bulk 3*d*-metal environment, where the usual description includes strong hybridization and crystal field effects. In a particular case, we indeed observe survival of significant orbital magnetism. This experimental observation is accompanied by *ab initio* theory which explains why orbital magnetism is quenched in Fe but survives in Co.

The samples were prepared by melting high-purity starting materials together in inert atmosphere or in UHV to give a master alloy that was then successively diluted to obtain the desired concentration. The alloys studied were *Au*V (1.5 at.%), *Au*Cr (1.0 at.%), *Au*Mn (1.0 at.%), *Cu*Mn (1.0 at.%), *Au*Fe (0.8 at.%), and *Au*Co (1.5 at.%). For a random alloy of 1.0 at.% impurity concentration in the Au host, the probability of two impurities being nearest neighbors is about 10%, and the probability of occurrence of still larger nearest-neighbor clusters is vanishingly small. Calculations [9] for the Au host indicate that one 3*d* nearest neighbor changes the magnitudes of the 3*d* local moments only minimally ($<10\%$ including orbital effects), while more distant neighbors have a negligible effect (exchange coupling of nearest-neighbor moments may, however, occur). We thus expect that our XAS and XMCD spectra are representative of single 3*d* impurities in the Au host matrix. After the desired concentration was reached, the alloys were annealed for ca. 48 h near the melting point, then quenched

rapidly to room temperature. They were characterized by x-ray diffraction and SQUID magnetometry. The magnetic characteristics (glass temperature T_G, magnetic moment per atom) were consistent with literature values. After installation in the UHV measuring chamber, they were sputtered with Ar ions at 0.6 kV for 1–2 h while their XAS spectra in the region of the oxygen K and $3d$ $L_{\mathrm{II,III}}$ edges were registered. Sputtering was continued until all traces of oxidation and compound formation had been eliminated from the spectra (except for the case of AuV where apparently internal oxidation or formation of intermetallic compounds had occurred and the dichroism signal was very weak). The AuV data were accordingly not used for further analysis.

The XAS experiments were performed on the new ID8 beam line/XMCD station at ESRF [10]. The $3d$ paramagnetic moments were aligned in external fields B_0 of up to 7 T at temperatures down to 4 K; care was taken to keep the measurement temperature above the glass temperature determined by SQUID magnetometry. The circularly polarized photon beam impinged on the disk-shaped samples at 90° incidence. Fluctuations in beam intensity were normalized using the photocurrent signal from a gold grid, and the XAS signal was obtained as the total electron yield from the samples. XMCD measurements were carried out for the four possible combinations of the B_0 and beam polarization directions under conditions which maximized the sample magnetization (magnetic saturation could not be attained in these Kondo systems at the available magnetic fields). Magnetization curves were also obtained by varying B_0 at constant temperature. Figure 1 shows the XAS spectra normalized to unity at the preedge and the corresponding XMCD curves obtained from them. Note that the $L_{\mathrm{II,III}}$ edge jumps of the $3d$ impurities are in the range of 0.1% relative to the background signal. All the XAS spectra were normalized to the absorption of a clean gold sample (measured at the corresponding external field and temperature) in order to remove the superposed background originating from the host material and the transmission function of the beam line. In spite of the XAS background, excellent XMCD spectra were obtained on subtraction.

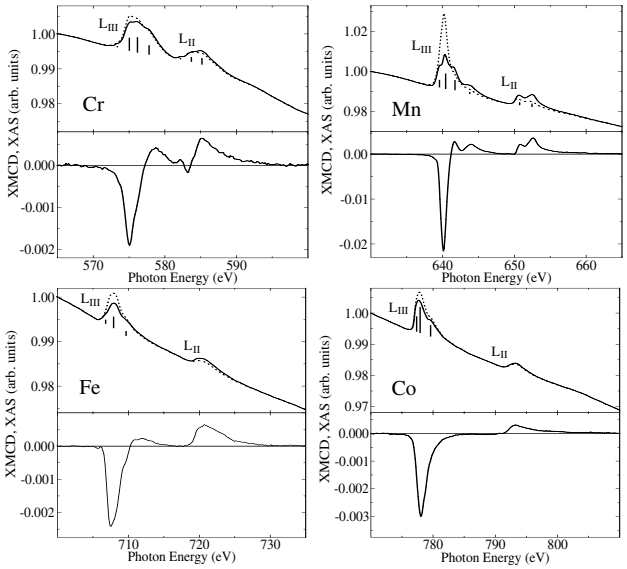

FIG. 1. XAS spectra (upper plots) and difference (XMCD) spectra (lower plots) of the $3d$ elements Cr-Co in the $L_{\mathrm{II,III}}$ spectral region. Note the strongly reduced relative intensity at the L_{II} edge of Co, indicative of its enhanced orbital moment.

In the atomic limit, the $L_{\mathrm{II,III}}$ XAS reveal sharp multiplet structures [3,11] which are a sensitive fingerprint for the atomic configuration. However, these prominent features diminish in the shallow d bands in the solid state. While multiplets are consequently absent in bulk XAS, they appear clearly in the spectra of the $3d$ impurities in a Au matrix, albeit obscured by hybridization effects. This manifests the nature of impurities, which bridge the gap between the atomic and the solid states. Here, the absorption fine structure is an indicator of the degree of hybridization of the d orbitals with the Au host bands. The role of crystal field effects and hybridization can be assessed from the branching ratio, which is the fraction of the $2p_{3/2}$ transition channel (L_{III} edge). The maximum branching ratio is obtained for the Hund's rule ground state and decreases successively with increasing crystal field and hybridization effects, which lower the spin polarization of the $3d$ states [12]. Relative to the bulk metals, all branching ratios of the impurities determined from the averaged absorption spectra are considerably enhanced towards those of their atomic configurations [11], except for Co: values for the atom/impurity/bulk are 0.79/0.67/0.56, 0.76/0.79/0.67, 0.84/0.79/0.70, and 0.93/0.82/0.79 for Cr, Mn, Fe, and Co, respectively. This indicates the formation of large spin moments for Cr, Mn, and Fe impurities in the Au host as predicted by theory [13].

The orbital-moment contribution to the XMCD spectrum can be deduced from the ratio R of the L_{II} to L_{III} peak areas. For $R \approx -1$, the orbital moment is practically quenched, and it increases with increasing deviation from this value. The relative coupling of spin and orbital moments is antiparallel (parallel) for $R < -1$ ($R > -1$). A notable difference in R for Co and Fe impurities can be clearly seen in the corresponding XMCD spectra. This evidences a large orbital contribution to the magnetic moment of Co without invoking a sum rule analysis [14–16]. We have extracted the $L_{\mathrm{II,III}}$ peak areas of the XMCD signal and quantitatively evaluated the orbital to spin moment ratio according to

$$\frac{\mu_l}{\mu_s^{\mathrm{eff}}} = \frac{2}{3}\,\frac{1+R}{1-2R}. \qquad (1)$$

This ratio is an excellent indicator of the relative strength of orbital magnetism and can be compared directly to the

ratio obtained from theory. The spin moment is denoted here by μ_s^{eff}, allowing for the contribution of the magnetic dipole term $\langle T_z \rangle$ and the deviation from the spin sum rule due to the $2p$–$3d$ core hole interaction in the light $3d$ elements [17]. The results are shown in Fig. 2, where μ_l/μ_s^{eff} is plotted vs electron number for the dilute $3d$ impurities in Au host and compared with theory [13] for dilute $3d$ impurities in noble metal hosts obtained in a real-space linear muffin-tin orbital calculation in the atomic sphere approximation using the scalar relativistic approach and including spin-orbit coupling [18]. The calculations were performed both with and without orbital polarization (OP) [19], which in many cases probably overestimates the orbital contribution [20]. It can be seen from this figure that the tendencies predicted by theory, i.e., small negative orbital moments ($R < -1$) at the beginning of the $3d$ series, becoming positive ($R > -1$) in the second half of the series and very large for Co, are verified by the experimental results. The experimental value of μ_l/μ_s^{eff} for Co lies just between the theory predictions with and without OP, confirming the statement that the calculation without OP underestimates the orbital contribution, while the current OP scheme overestimates it. We emphasize that the large value of the orbital/spin ratio found here for Co, $\mu_l/\mu_s^{\text{eff}} \simeq 0.34$, is considerably greater than those observed in bulk systems, e.g., 0.091 in Co metal [14], but less than those seen in surface layers, e.g., 0.6–0.9 for 1.5% monolayers of Co on Na and K [3]. The smaller values and variations found for the $3d$ impurities Cr-Fe are in general agreement with theory within the experimental and theoretical uncertainties. The values of the ratio μ_l/μ_s^{eff} obtained are set out in Table I.

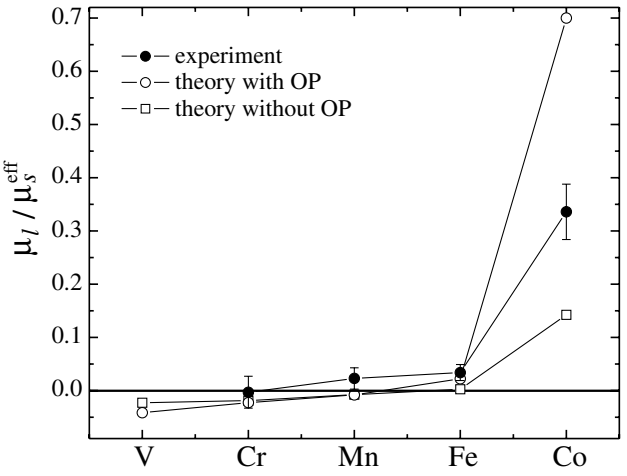

FIG. 2. Systematics of the orbital/effective spin moment ratio for the $3d$ series as impurities in the Au host. The experimental results from XMCD (filled points) are compared with theory with (open circles) and without (open squares) the OP correction. The true ratio μ_l/μ_s lies within the error limits. In particular, for Co the uncertainty of the $\langle T_z \rangle$ contribution is scaled from the free atom (d^8) to the impurity in the ratio of their orbital moments. Note that taking the $\langle T_z \rangle$ term into account would lead to a ~20% higher μ_l/μ_s ratio.

The systematics of $3d$ orbital moments can be approximated to first order (spin-orbit coupling treated as a weak perturbation) by the difference of the spin-split local density of states at the Fermi level $n^{\uparrow,\downarrow}(E_F)$ [21]. For Mn, Fe, and Co the virtual bound state in the minority band is consecutively filled, while the majority band is almost full. Therefore, the magnitude of the orbital moment can be basically estimated from $n^{\downarrow}(E_F)$ of the virtual bound state. Thus the formation of an orbital moment depends sensitively on hybridization with the host, influencing the width and the relative energy position of the virtual bound state. The large value of $n^{\downarrow}(E_F)$ and the related large orbital contribution is less affected for Co dissolved in Au or Ag. However, the stronger hybridization of Fe in Au relative to Fe in Ag leads to a broadening and a decrease of $n^{\downarrow}(E_F)$ at the Fermi energy. The Fe orbital moment is thus 10 times smaller in the Au matrix than that of Co, adjacent in the $3d$ series.

In Fig. 3, $L_{\text{II,III}}$ XMCD spectra are shown for Mn dissolved in a Cu and a Au matrix, illustrating the influence of the host matrix on the local electronic structure. The spectra were normalized to unity at the L_{III} edge in order to emphasize the effects of the host. The overall line shape of the XMCD (and XAS) signal persists; however, the structural details are sharpened for Mn in Au. This can be understood by considering the stronger hybridization of the impurity with Cu, favored by its smaller lattice constant than the Au host. Moreover, one sees a relative enhancement of the L_{II} XMCD signal for Mn in Cu. The resulting ratio $R \approx -1$ shows that the stronger hybridization of Mn with Cu leads to a smaller value of the μ_l/μ_s^{eff} ratio in the Cu host; cf. Table I.

In conclusion, the present work gives the first evidence that in contrast to textbook arguments about the quenching of orbital moments, the orbital moment of $3d$ impurities may survive to a large extent in a nominally cubic host material. This effect depends on (i) the hybridization between the impurity and the host material, here Au (for

TABLE I. Experimental values of R and the derived orbital/spin magnetic moment ratios for $3d$ impurities in noble metals. The applied field was 7 T, and temperatures T are in K.

Alloy	R	T	μ_l/μ_s^{eff}
*Au*Cr (1.0 at.%)	−1.01	18.7	−0.003(30)
*Au*Mn (1.0 at.%)	−0.90	6.8	+0.023(20)
*Cu*Mn (1.0 at.%)	−0.94	6.8	+0.013(20)
*Au*Fe (0.8 at.%)	−0.86	7.2	+0.034(15)
*Au*Co (1.5 at.%)	−0.247	6.8	+0.336(52)

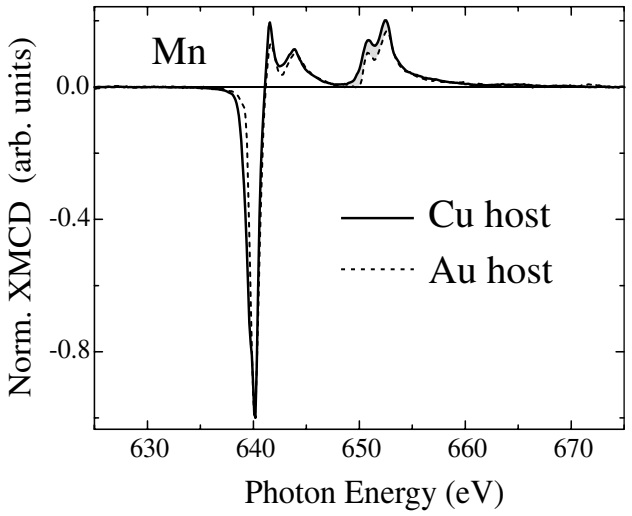

FIG. 3. $L_{II,III}$ XMCD spectra of Mn as a dilute impurity in Cu (solid line) and Au (dashed line). The ratio of peak areas in the L_{II} and L_{III} regions yields the orbital/spin moment ratio R.

Ag the situation would be different), and (ii) the filling of the $3d$ states of the impurity. Our theoretical results confirm the experimental finding that the larger filling for Co and energy separation of the valence band of Au causes the large orbital magnetism in Co and explains why the effect is small for the less-filled $3d$ states of adjacent Fe. Consequently, local orbital magnetic moments may be significant not only on surfaces, but can also occur in bulk materials of cubic symmetry.

We are grateful to Dr. O. Beutler, Dr. R. Kirsch, and Dr. M. Gierlings for assistance with sample preparation and magnetometry. We thank the staff of ESRF for support and assistance with the experiments. This work was funded by the BMBF (Grant No. O5KS1 KEB4) and the DFG in Germany and by the CNPq in Brazil.

*Electronic address: brewer@physik.fu-berlin.de

[1] *Magnetism: Magnetic Properties of Metallic Alloys*, edited by G.T. Rado and H. Suhl (Academic Press, New York, 1973), Vol. V.
[2] J. Friedel, Nuovo Cimento Suppl. **7**, 287 (1958).
[3] P. Gambardella *et al.*, Phys. Rev. Lett. **88**, 047202 (2002).
[4] P. Gambardella *et al.*, Science **300**, 1130 (2003).
[5] A. Narath and D. C. Barham, Phys. Rev. B **7**, 2195 (1973).
[6] J. Boysen, W. D. Brewer, and J. Flouquet, Solid State Commun. **12**, 1095 (1973).
[7] P. Steiner and S. Hüfner, Phys. Rev. B **12**, 842 (1975).
[8] D. Riegel and K.-D. Gross, in *Nuclear Physics Applications in Materials Science*, edited by E. Recknagel and J. C. Soares, NATO-ASI, Series E, Vol. 144 (Kluwer Academic, Dordrecht, 1988), p. 327.
[9] S. Frota-Pessôa, J. Magn. Magn. Mater. **226–230**, 1021 (2001).
[10] See http://www.esrf.fr/exp_facilities/ID8/ID8.html.
[11] G. van der Laan and B. T. Thole, Phys. Rev. B **43**, 13 401 (1991).
[12] B. T. Thole and G. van der Laan, Phys. Rev. B **38**, 3158 (1988).
[13] S. Frota-Pessôa, Phys. Rev. B **69**, 104401 (2004).
[14] C. T. Chen *et al.*, Phys. Rev. Lett. **75**, 152 (1995).
[15] B. T. Thole *et al.*, Phys. Rev. Lett. **68**, 1943 (1992).
[16] P. Carra *et al.*, Phys. Rev. Lett. **70**, 694 (1993).
[17] A. Scherz *et al.*, Phys. Rev. B **66**, 184401 (2002).
[18] S. Frota-Pessôa, Phys. Rev. B **46**, 14570 (1992); S. B. Legoas *et al.*, Phys. Rev. B **61**, 10 417 (2000).
[19] O. Eriksson *et al.*, Phys. Rev. B **42**, 2707 (1990).
[20] I. Cabria *et al.*, Phys. Rev. B **65**, 054414 (2002).
[21] H. Ebert *et al.*, J. Appl. Phys. **67**, 4576 (1990).